Electronic Supplementary Information (ESI)

Protein-Structure-Dependent Spectral Shifts of Near-Infrared Photoluminescence from Locally Functionalized Single-walled Carbon Nanotubes Based on Avidin–biotin Interactions

Yoshiaki Niidome [a], Rie Wakabayashi [a], Masahiro Goto [a,b], Tsuyohiko, Fujigaya [a,c,d]* and Tomohiro Shiraki [a,c]*

[a] *Department of Applied Chemistry, Graduate School of Engineering, Kyushu University, 744 Motooka, Nishi-ku, Fukuoka 819-0395, Japan.*

[b] *Center for Future Chemistry (CFC), Kyushu University, 744 Motooka, Nishi-ku, Fukuoka 819-0395, Japan.*

[c] *International Institute for Carbon-Neutral Energy Research (WPI-I2CNER), Kyushu University, 744 Motooka, Nishi-ku, Fukuoka 819-0395, Japan.*

[d] *Center for Molecular Systems (CMS), Kyushu University, 744 Motooka, Nishi-ku, Fukuoka 819-0395, Japan.*

email: shiraki.tomohiro.992@ m.kyushu-u.ac.jp; fujigaya.tsuyohiko.948@ m.kyushu-u.ac.jp

Materials: Single-walled carbon nanotubes (SWCNTs) (CoMoCAT, (6,5)-rich), carboxymethyl cellulose sodium salt (Na-CMC), 20 wt% poly(diallyldimethylammonium chloride) (PDDA) solution, acetonitrile (AN), D_2O, bovine serum albumin (BSA), and 2-propanol (IPA) were purchased from Sigma-Aldrich Co., LLC. NH_2–PEG_{11}–biotin, diisopropyl phosphite (DIPP), 4-methoxybenzenediazonium tetrafluoroborate, 3-aminopropyltriethoxysilane (APTES), and sodium dodecylbenzenesulfonate (SDBS) were obtained from Tokyo Chemical Industry Co., Ltd. Methanol and *N,N*-dimethylformamide (DMF) were purchased from Dojindo Laboratories. Ethanol (EtOH), tetrahydrofuran (THF), NaOH, neutravidin (NAV), streptavidin (SAV), and avidin (AV) were purchased from Wako Pure Chemical Industries, Ltd. Fetal bovine serum (qualified, USDA-approved regions) were obtained from Gibco (thermofisher) and filtered prior to use. All the chemicals were used without further purification otherwise stated. Further, 4-formylbenzene diazonium tetrafluoroborate (CHO-Dz) was synthesized following a previously reported procedure. [R1]

Instrumentation: Photoluminescence (PL) spectra were measured using a HORIBA JOBIN YVON spectrofluorometer (FluorologR-3 with FluorEssence). Quartz cells with a 0.20-cm path length were employed for the optical measurements. MilliQ water was obtained from an ultrapure water system equipped with an Elix-5 kit (Millipore). For the preparation of the nanotube dispersions and polymer wrapping treatments, a bath-type sonicator (BRANSON, CPX5800H-J), a tip-type sonicator (Tomy Seiko, UD-200), an ultracentrifuge (Hitachi, Himac CS 100 GXL), a centrifuge (KUBOTA, KN-70) and a freeze dryer (EYELA, FDU-1200) were used.

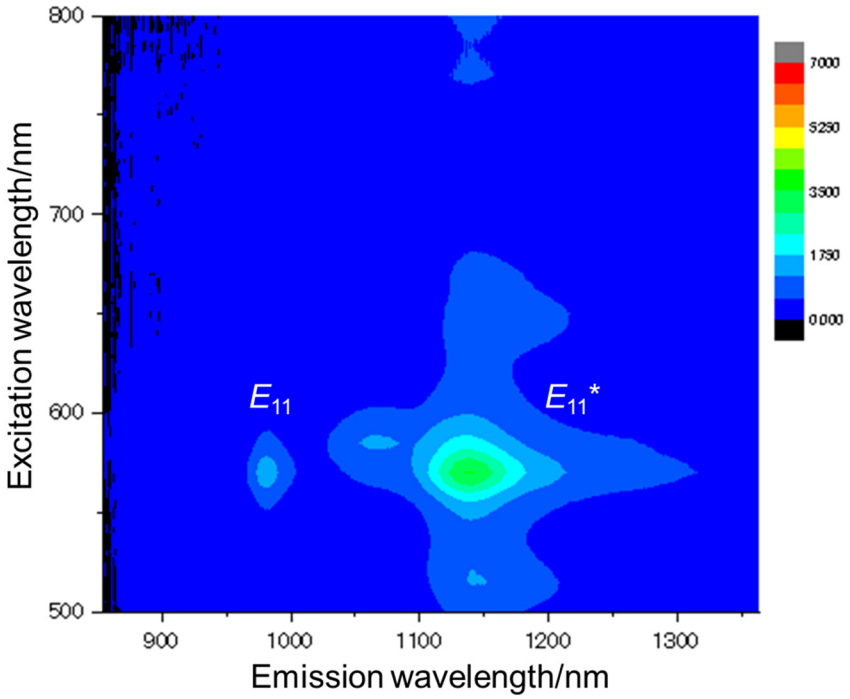

Fig. S1 PL mapping image of lf-SWCNTs-CHO/SDBS.

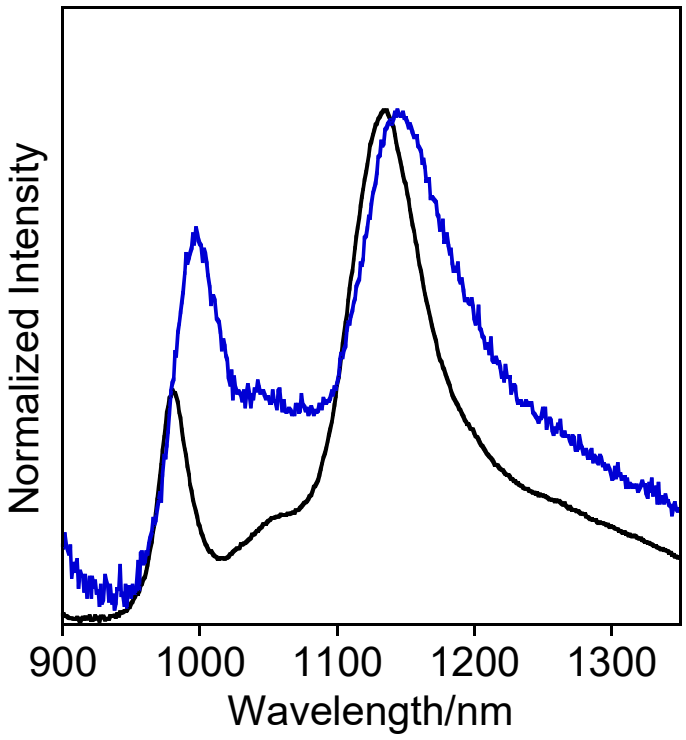

Fig. S2 Normalized PL spectra of lf-SWCNTs-b solubilized by SDBS (black) and Na-CMC (blue) in D_2O. λ_{ex} = 570 nm.

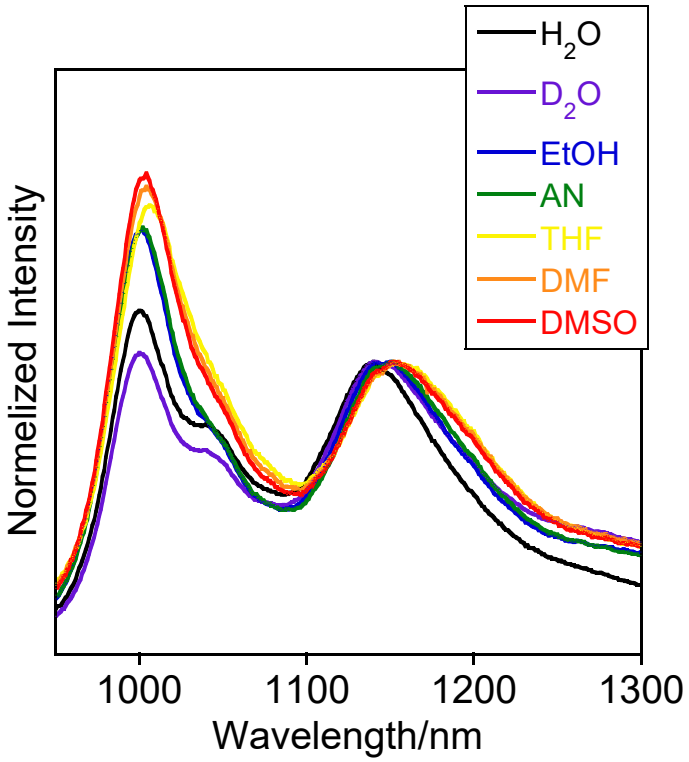

Fig. S3 Normalized PL spectra of lf-SWCNTs-b/Na-CMC/PDDA immobilized on quartz substrates, which were immersed in each solvent. λ_{ex} = 580 nm.

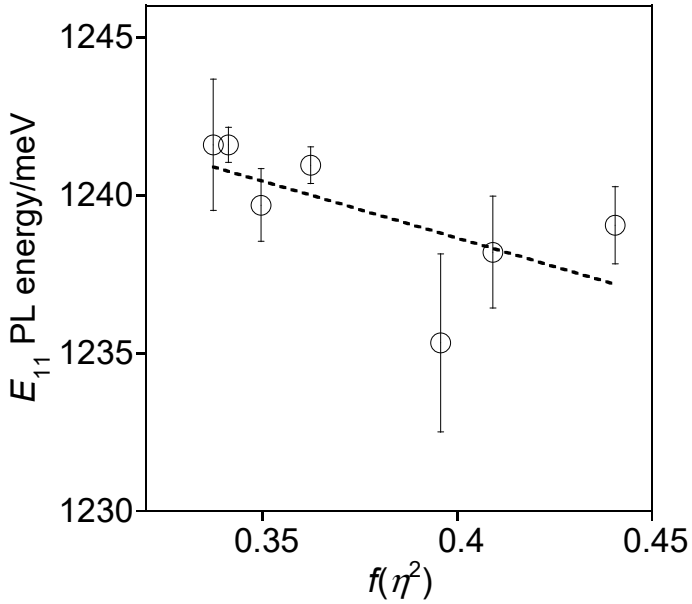

Fig. S4 Plot of the E_{11} PL energies against $f(\eta^2)$. The dotted line was obtained by the linear approximation method. Error bars are standard deviations of technical triplicates.

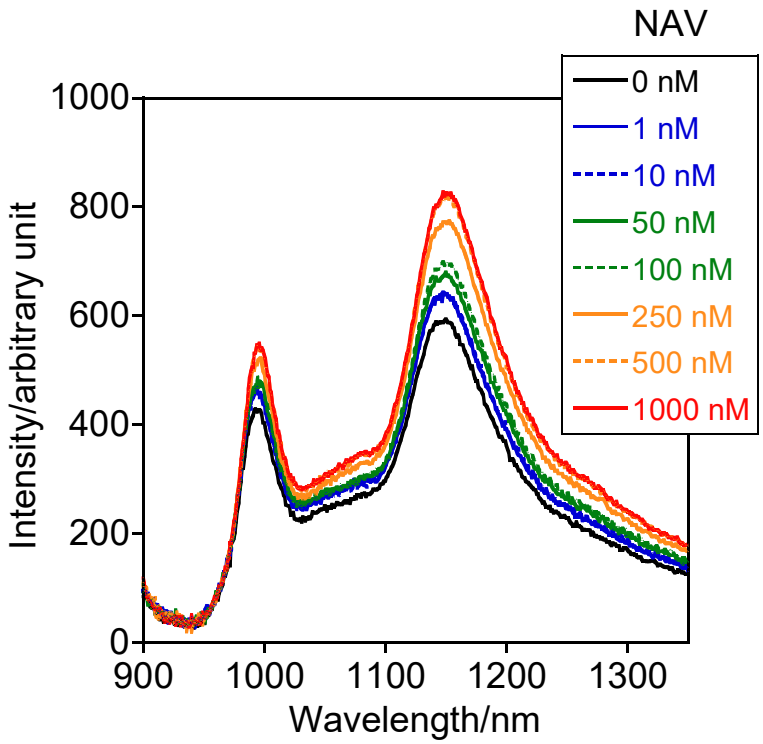

Fig. S5 PL spectra of lf-SWCNTs-b after conjugation with NAV. λ_{ex} = 580 nm.

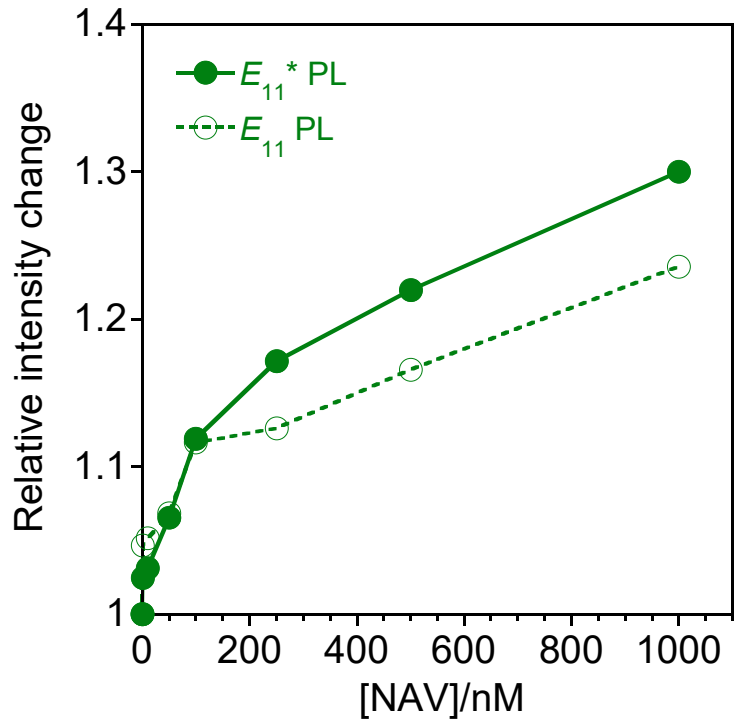

Fig. S6. Plot of the relative intensity changes of E_{11}* PL and E_{11} PL against NAV concentrations.

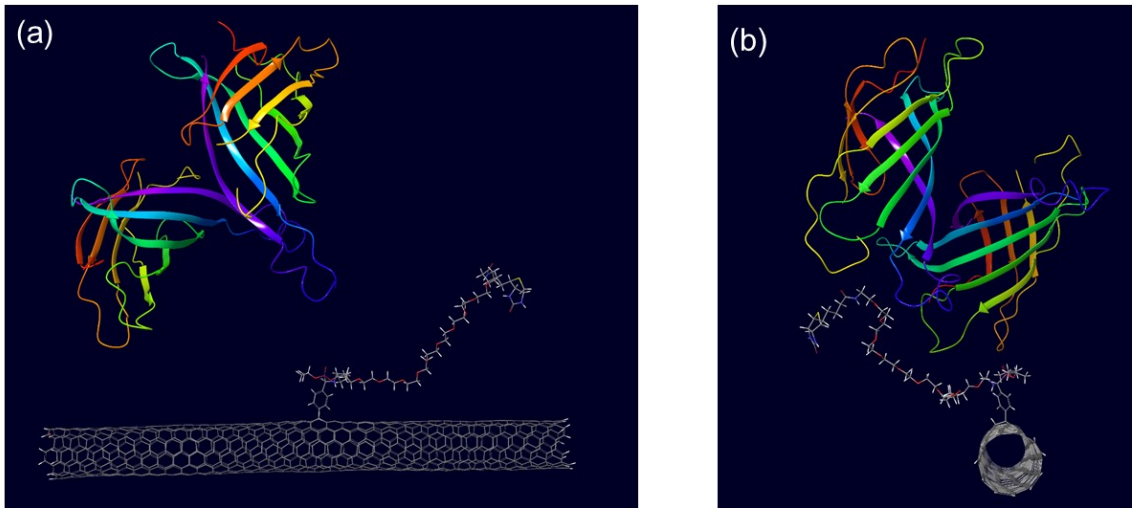

Fig. S7 Three-dimensional modeling images of lf-SWCNT-b and AV (PDB:1VYO): (a) a front view and (b) a side view.

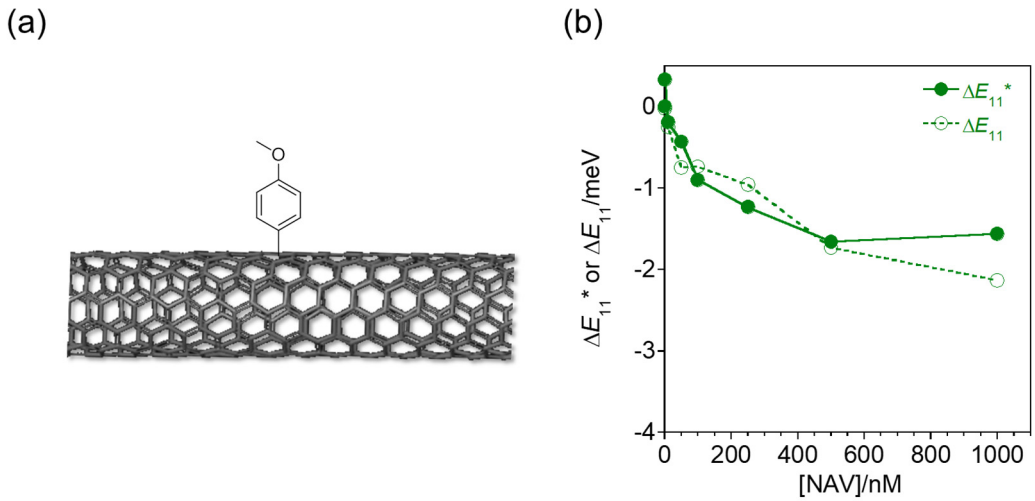

Fig. S8 (a) Schematic image of lf-SWCNTs-OCH_3. (b) Plots of ΔE_{11}* and ΔE_{11} for lf-SWCNT-OCH_3 conjugation with NAV. The average values of technical duplicates are shown.

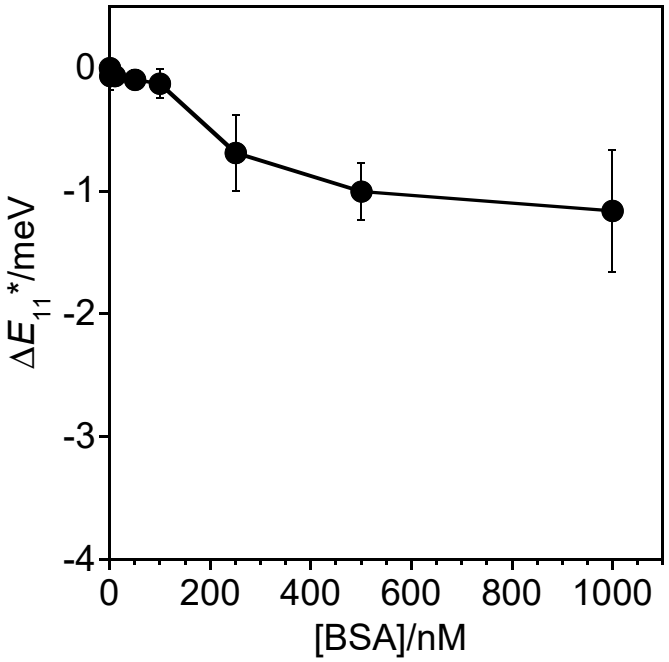

Fig. S9 Plots of the ΔE_{11}* of lf-SWCNTs-b as a function of the BSA concentration. Error bars are standard deviations of technical triplicates.

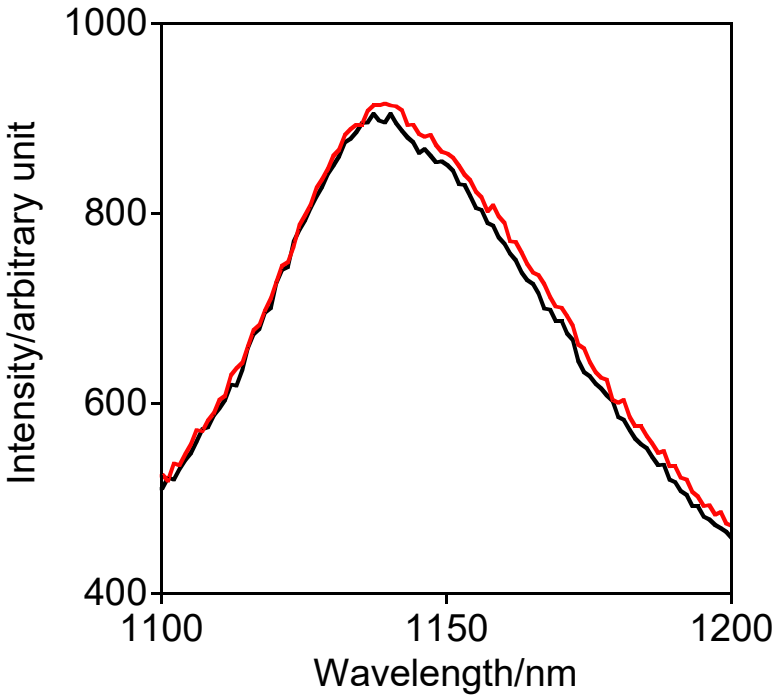

Fig. S10 PL spectra of lf-SWCNTs-b/Na-CMC in 1 % FBS solutions without (black) and with (red) the NAV addition (1000 nM). λ_{ex} =580 nm.

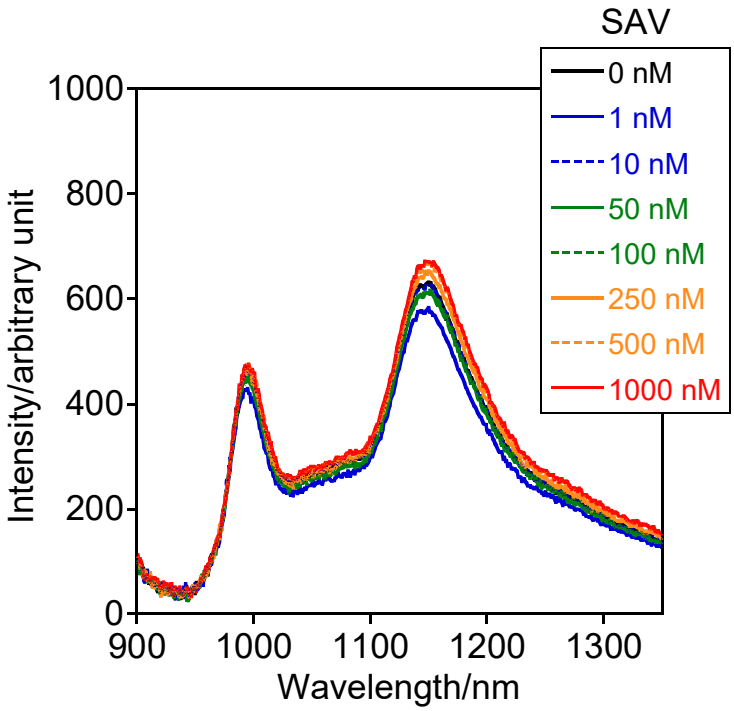

Fig. S11 PL spectra of lf-SWCNTs-b after conjugation with SAV. λ_{ex} = 580 nm.

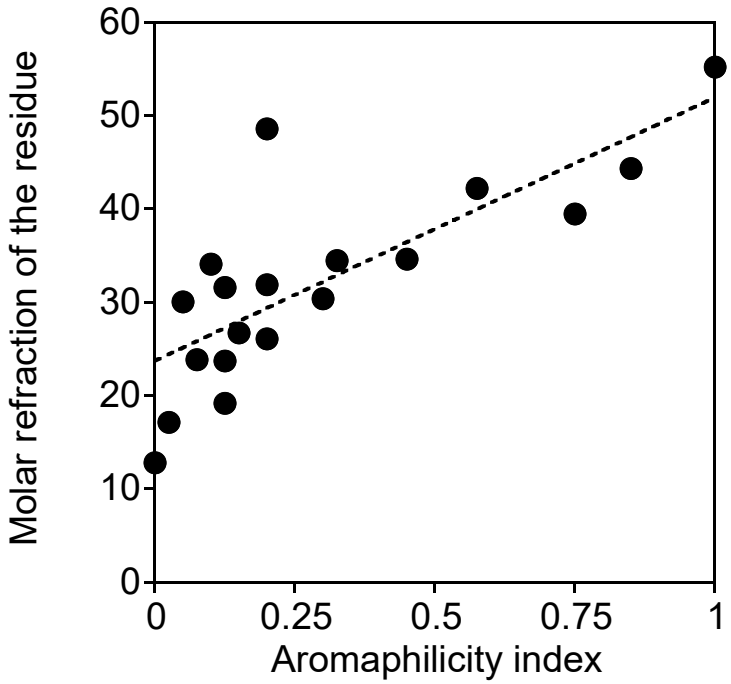

Fig. S12 Plot of the molar refraction of the residue against the aromaphilicity index of the amino acids. The dotted line was obtained by the linear approximation method (R^2 = 0.617). Numerical data were obtained from Refs. R2 and R3.

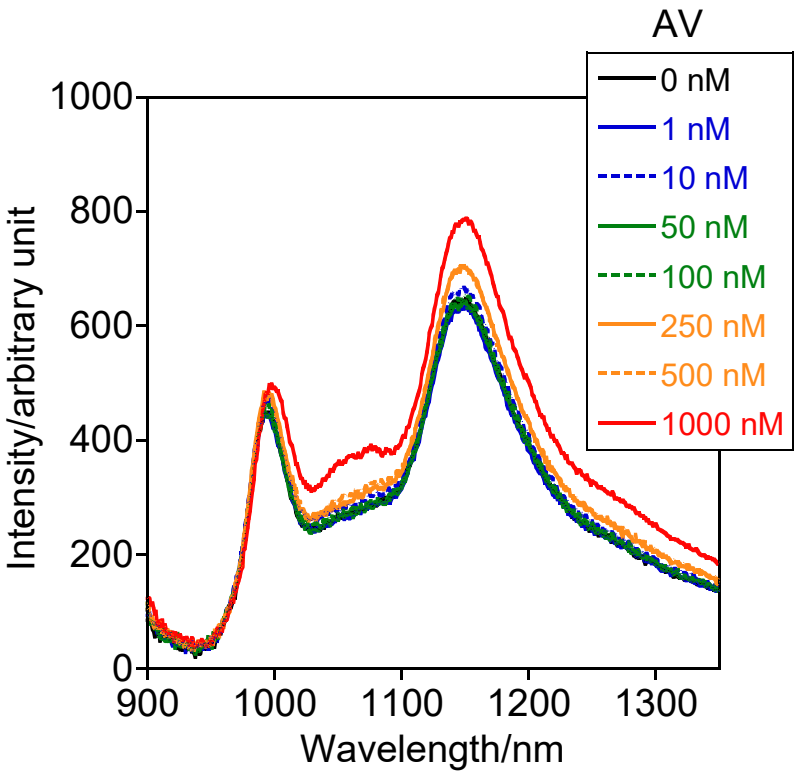

Fig. S13 PL spectra of lf-SWCNTs-b after conjugation with AV. λ_{ex} = 580 nm.

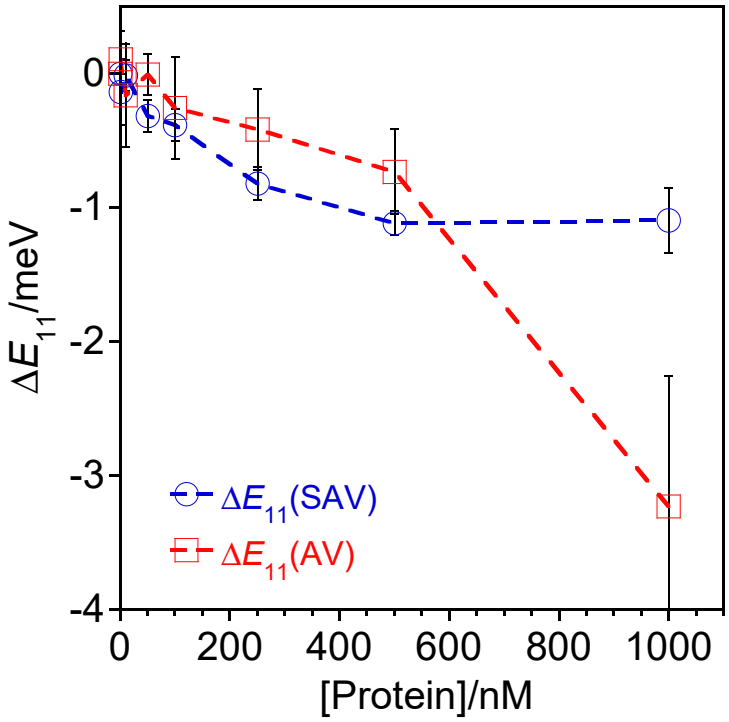

Fig. S14 ΔE_{11} of lf-SWCNTs-b against the AV (red) and SAV (blue) concentrations. Error bars are standard deviations of technical triplicates.

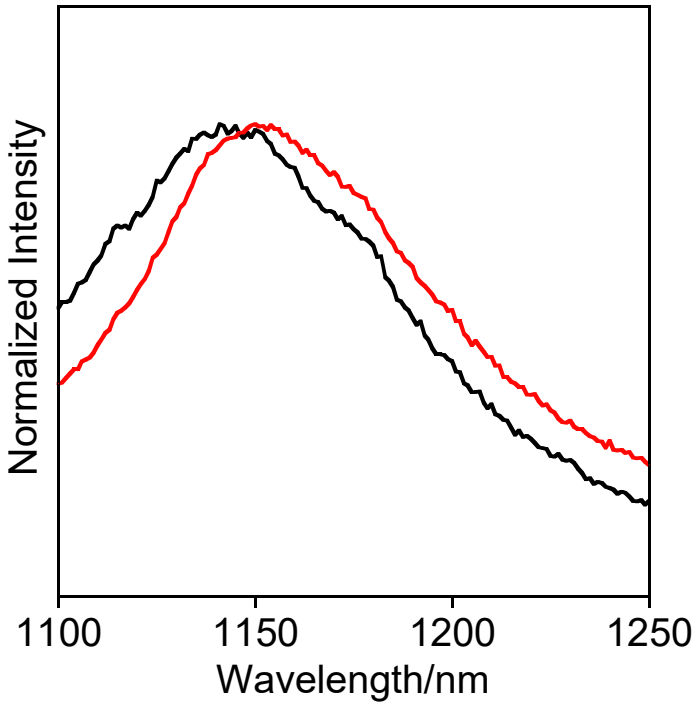

Fig. S15 Normalized PL spectra of lf-SWCNTs-b/Na-CMC on the APTES-modified substrate before (black) and after (red) immersion in a 1000 nM SAV solution. λ_{ex} =580 nm.

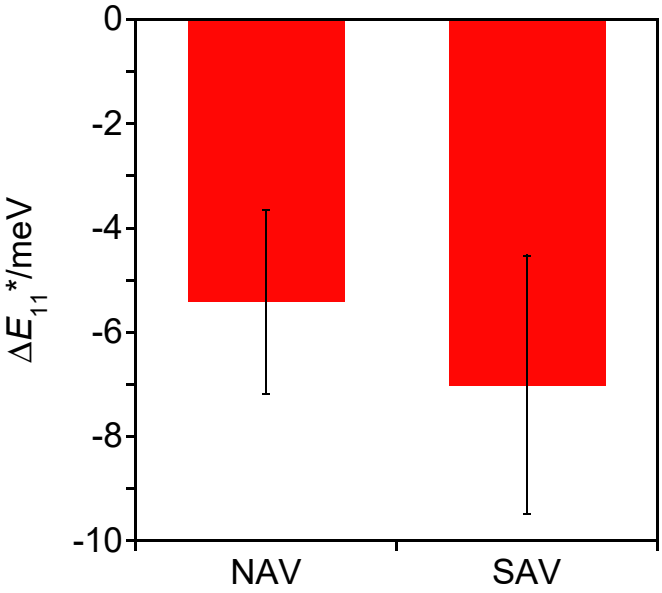

Fig. S16 ΔE_{11}* of lf-SWCNTs-b/Na-CMC on the substrate, after dipping in a NAV solution, where protein concentration is 1000 nM. Error bars are standard deviations of technical triplicates.

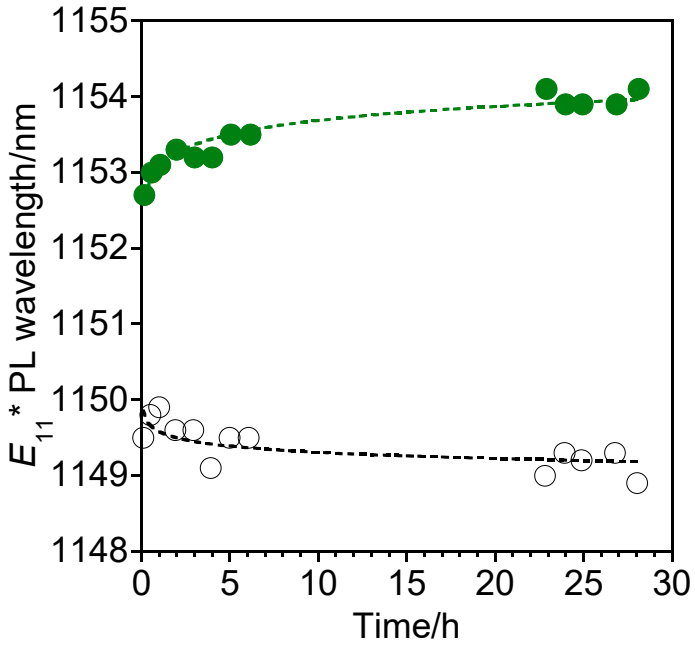

Fig. S17. Time-dependent wavelength changes in the E_{11}* PL for lf-SWCNTs-b without (−, black) and with (+, green) NAV.

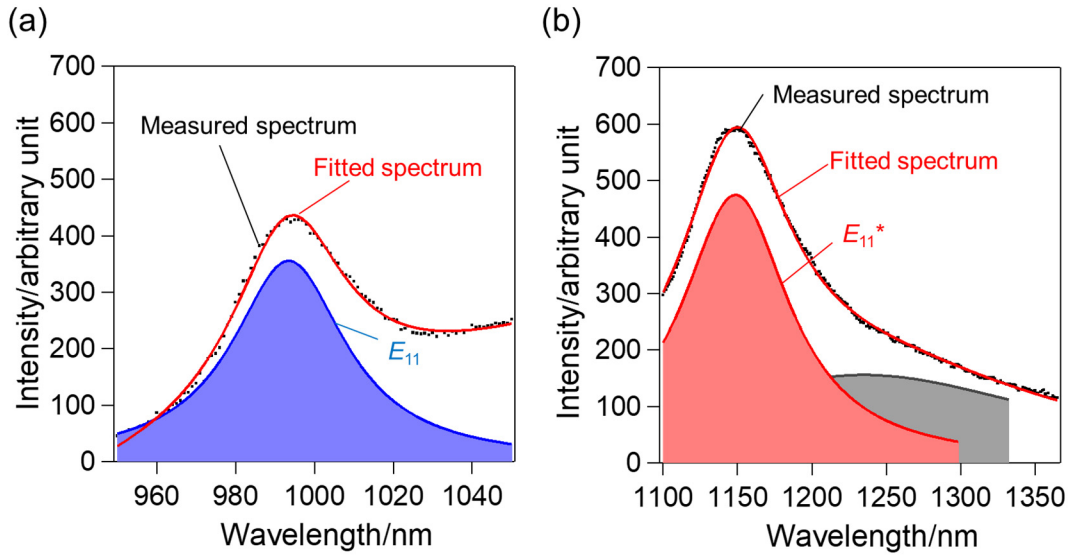

Fig. S18. Deconvoluted PL spectra of lf-SWCNTs-b/Na-CMC in D_2O solutions for (a) E_{11} PL and (b) E_{11}* PL.

Table S1 Properties of the used solvents for this study.

	Refractive index[R4,R5] η	Induction polarity parameter $f(\eta^2)$
D_2O	1.328	0.338
H_2O	1.333	0.341
EtOH	1.361	0.362
AN	1.344	0.350
THF	1.405	0.394
DMF	1.431	0.411
DMSO	1.479	0.442

References for ESI

R1. T. Shiraki, T. Shiga, T. Shiraishi, H. Onitsuka, N. Nakashima and T. Fujigaya, *Chem. Eur. J.*, 2018, **24**, 19162–19165.

R2. T. L. McMeekin, M. Wilensky and M. L. Groves, *Biochem. Biophys. Res. Commun.,* 1962, **7**, 151–156.

R3. A. Hirano and T. Kameda, *ACS App. Nano Mater.*, 2021, **4**, 2486–2495.

R4. H. Odhner and D. T. Jacobs, *J. Chem. Eng. Date*., 2012, **57**, 166-168.

R5 D. R. Lide, CRC handbook of chemistry and physics the 84th edition.